Crystal Growth Kinetics of Theophylline Monohydrate

Naír Rodríguez-Hornedo[1,3] and Hsiu-Jean Wu[2]

Received September 7, 1990; accepted December 26, 1990

The crystal growth kinetics of theophylline monohydrate from aqueous buffered supersaturated solutions were investigated at 10, 20, 30, and 40°C. Crystallization experiments were carried out isothermally at pH 6. During growth the crystal count and size distributions were monitored *in situ*. The growth rate was evaluated from the rate of change of the size with time at a constant value of the size distribution. The growth rate is independent of the stirring rate and the activation energy for growth is higher than the value for simple diffusion, 14.3 and 4.4 kcal/mol, respectively. This indicates that crystal growth of theophylline monohydrate is controlled by a surface reaction mechanism rather than by solute diffusion in the bulk. The growth-rate dependence on the supersaturation was compared with crystal growth theories. The data are described by the screw dislocation model and by the parabolic law, suggesting a defect-mediated growth mechanism rather than a surface nucleation mechanism.

KEY WORDS: theophylline monohydrate; crystal growth; phase transition; growth kinetics.

INTRODUCTION

Transformations between solid phases are a very important aspect in the development of a dosage form (1–9), since the presence of a metastable phase during processing or in the final product often leads to instability of drug release. It is thus crucial to understand the mechanism and kinetics of phase transformations and the factors that may influence them.

Anhydrous to hydrate transitions are frequently encountered in pharmaceutical systems, e.g., ampicillin (1,2), carbamazepine (3,4), and theophylline (5–10). De Smidt and co-workers (7) have shown that, during dissolution of anhydrous theophylline from a disk, the solid on the surface is transformed to the monohydrate form. The solubility of the anhydrous form exceeds the solubility of the hydrated form, below 60°C. They observed that the length of the transformation phase depended on the characteristics of the diffusion layer and concluded that theophylline monohydrate crystallizes from the supersaturated solution adjacent to the disk surface. Recent studies (8,9) show erratic dissolution rates of anhydrous theophylline from formulations prepared by wet granulation. These have been explained by the anhydrous-to-monohydrate transition. Similar observations have been reported with anhydrous carbamazepine (3). Anhydrous carbamazepine has a higher solubility than the dihydrate form, however, under some conditions carbamazepine dihydrate seems to dissolve faster than the anhydrous modification, due to the rapid crystallization of the dihydrate on the anhydrous form.

The emphasis of previous studies (1–11) has been to characterize the solid phase, to evaluate thermodynamic parameters associated with the phase transitions, and to determine the kinetics of a solid state transition where the solid phases are in contact with a vapor. Almost neglected is the possibility that the transformation can proceed by a solution-mediated mechanism, with dissolution of the metastable phase and growth of the stable phase.

A major goal of our work was to investigate the processes that occur during the anhydrous-to-hydrate transformation of theophylline crystals in a buffered solvent. These involve (i) dissolution of the anhydrous phase and (ii) nucleation and growth of the monohydrate crystals. The main objective of the work presented here was to study the growth kinetics of monohydrate theophylline crystals and the effect of temperature and stirring rate on the growth rate. We compared our results with the predictions of various crystal growth models to gain some insight about the underlying growth mechanism.

MATERIALS AND METHODS

Materials

Anhydrous theophylline was obtained from Sigma Chemical Company. Monohydrate theophylline crystals were prepared by crystallization from phosphate buffer (pH 6) that was supersaturated by dissolving the anhydrous form. Monohydrate crystals were dried at room temperature and stored over a saturated solution of sodium bromide (relative humidity, 60%). The water used in this study was filtered through a double-deionized purification system (Milli Q Water System from Millipore Company). Phosphate buffer (pH 6) was prepared from 0.067 *M* potassium phosphate monobasic solution and 0.067 *M* sodium phosphate dibasic solution. The ionic strength of the buffer was adjusted to 0.15 *M* with potassium chloride. These reagents were purchased from Aldrich Chemical Company. All solutions were filtered through a 0.45-μm filter prior to use.

Assay and Identification

Theophylline concentration in solution was measured by UV spectrophotometry with a Beckman DU-8 spectrophotometer at 270 nm. An IR spectrophotometer (Beckman IR-33) was used to determine the IR spectra of anhydrous and monohydrate theophylline crystals. Differential scanning calorimetry was done with a Dupont 1090 thermal analyzer.

Solubility Measurement

The solubility of theophylline monohydrate was measured over the temperature range 8 to 40°C, in 0.067 *M* phosphate buffer, pH 6, with an ionic strength of 0.15 *M*. Equilibrium was approached from an undersaturated solution and from a supersaturated solution. In the former, excess mono-

[1] College of Pharmacy, The University of Michigan, Ann Arbor, Michigan 48109-1065.
[2] College of Pharmacy, The University of Arizona, Tucson, Arizona 85721.
[3] To whom correspondence should be addressed.

0724-8741/91/0500-0643$06.50/0

hydrate theophylline crystals were added to 100 ml of buffer and stirred in a jacketed beaker. Aliquots were taken at various times and assayed until the system reached equilibrium, at 24 hr. In the latter, supersaturation with respect to the monohydrate form was achieved by dissolving anhydrous theophylline. The monohydrate crystals nucleated and grew, until the concentration reached a constant value. The resulting data pair converged to the solubility value of the monohydrate modification. The temperature was controlled with a refrigerated circulating bath (Neslab, RTE-400) to within 0.3°C.

Crystallization System and Procedure

Crystallization experiments were carried out isothermally in a 250-ml jacketed beaker at 10, 20, 30, and 40°C. The crystal count and size distribution (CSD) were obtained *in situ* with an Elzone 180XY particle counter (Particle Data Laboratories, Elmhurst, IL). Crystal sizes (volume equivalent size) within the range of 12 to 100 μm were measured using a 300-μm orifice size. The system was stirred with a glass impeller at 400, 700, and 1200 rpm.

Solutions supersaturated with respect to theophylline monohydrate (200 ml) were prepared at various concentrations. Supersaturation was created by cooling a saturated solution and adding a small volume of a highly concentrated theophylline solution (60 mg/ml) in 0.1 *N* sodium hydroxide. This did not significantly change the ionic strength or the pH of the system. The crystallizer was allowed to reach the desired temperature and a 0.5-ml aliquot of suitably sized theophylline monohydrate seed crystals was added. The CSD was monitored during an experiment and small volumes of solution assayed for theophylline concentration.

Theophylline Monohydrate Seeds

Phosphate buffer, pH 6, saturated with theophylline monohydrate at 25°C was chilled in an ice bath (−10°C) to 0°C with constant stirring. The suspension was filtered after the crystal seeds reached the desired size. The seeds were resuspended and aged in saturated buffer for a period of 2 weeks at room temperature. The seeds were identified by IR spectroscopy and the number per milliliter and CSD measured. The seed suspension had 76 mg monohydrate crystals in 1 ml.

Data Analysis

The CSD on a number basis was obtained as a function of time during an experiment (Fig. 1). The growth rate is independent of crystal size, since successive size distribution curves remained parallel. The growth rate, G, was evaluated from the rate of change of the size, L, with time, t, at a constant value of the size distribution function, F (12):

$$G = \left(\frac{dL}{dt}\right)_F \cong \left(\frac{\Delta L}{\Delta t}\right)_F \qquad (1)$$

The growth rate over a time interval was related to the supersaturation. Thus the growth rate dependence on the supersaturation was obtained.

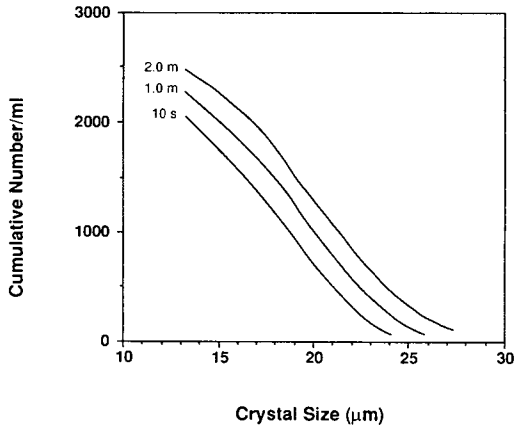

Fig. 1. Crystal size distributions of theophylline monohydrate during growth at 10°C and initial supersaturation of 0.42.

RESULTS AND DISCUSSION

Theophylline monohydrate is the stable solid phase in the buffer solution and temperature range studied. The temperature dependence of the solubility, shown in Fig. 2, is described by

$$\ln (S_H) = 14.89 - 3907\ (1/T) \qquad (2)$$

where S_H is the solubility of the monohydrate form (mg/ml) and T is the absolute temperature.

The growth rate dependence on the theophylline concentration may provide some insight to the underlying growth mechanism by which molecules build up the crystal. The values found for the growth rate, G, are plotted in Fig. 3 as a function of the supersaturation. The supersaturation is defined as $\sigma = (C - S)/S$, where C is the concentration of theophylline in solution and S is the solubility. Figure 4 shows a photograph of theophylline monohydrate crystals.

We compared our results with the predictions of various crystal growth models. These models fall into four main categories depending on the rate-limiting step assumed: (a) solute transport within the bulk solution phase to the crystal surface, (b) uniform attachment of growth units to a surface that is rough on a molecular scale, (c) nucleation of two-

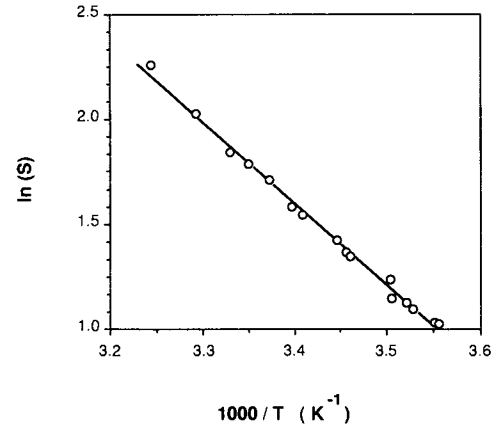

Fig. 2. Solubility of theophylline monohydrate in pH 6 buffer, plotted according to Eq. (2).

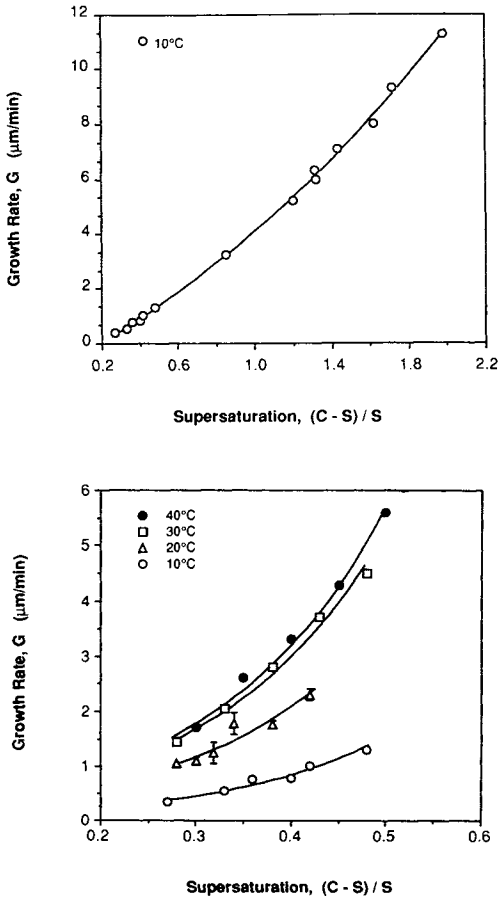

Fig. 3. Growth rates of theophylline monohydrate crystals in phosphate buffer, pH 6.

dimensional clusters on the surface, which expand and merge to form new layers, and (d) spreading of layers from a screw lattice dislocation which acts as a continuous source of steps.

If the equilibrium at the crystal face is sufficiently rapid so as not to be involved in the rate-limiting step, the crystallization would be controlled by the solute transport. The rate of crystallization would be expected to follow Ficks's law of diffusion and G is given by (13)

$$G = \frac{DV(C - S)}{\delta} \tag{3}$$

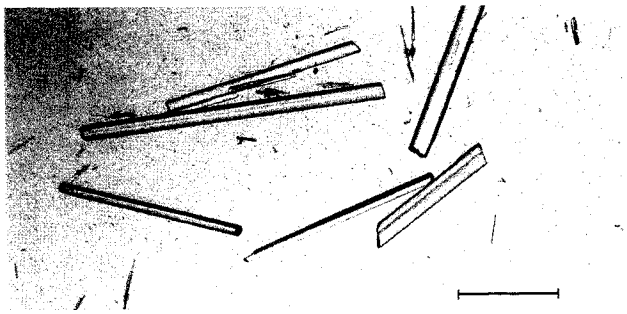

Fig. 4. Optical micrograph of theophylline monohydrate crystals. Marker represents 200 μm.

where D is the solute diffusion coefficient, V the molecular volume, and δ the boundary layer thickness. The observed growth rate of monohydrate theophylline crystals is more than an order of magnitude smaller than the growth rate calculated from Eq. (3). Furthermore, the growth rate was found to be independent of stirring rate in the range of 400 to 1200 rpm. These studies were done at 10°C (σ = 0.85) and at 20°C (σ = 0.34). These results indicate that the rate of crystallization is not controlled by solute transport in the bulk. Similar observations have been made in other systems (12,14).

If the crystal surface is rough on a molecular scale, it provides many uniformly distributed active sites for attachment of a molecule. For this model the growth rate is proportional to the driving force (15),

$$G = k_1 C \ln(C/S) \tag{4}$$

where

$$k_1 = \frac{DV}{d}$$

k_1 is a constant that determines the maximum growth rate for a given system and d is the molecular diameter. This growth mechanism leads to rounded crystal surfaces, whereas theophylline monohydrate crystals exhibited perfectly flat faces in the supersaturation range studied. Furthermore, Eq. (4) does not describe the concentration dependence of G that we observed.

When crystal faces are smooth, growth can occur by a two-dimensional nucleation mechanism or by a spiral growth mechanism.

In the case of two-dimensional nucleation, growth takes place by attachment of molecules to the edge of the nucleus on the surface. The growth rate is exponentially dependent on the driving force (15),

$$G = k_2 C^{1/3} [\ln (C/S)]^{5/6} \exp\left[- \frac{\pi\gamma^2}{3(k_B T)^2 \ln (C/S)} \right] \tag{5}$$

where

$$k_2 = \left(\frac{2\pi}{3}\right)^{1/3} \frac{2D_S n_S \upsilon}{\lambda a}$$

γ is the molecular surface energy of the crystal solution interface, k_B is Boltzmann's constant, D_s is the surface diffusion coefficient, λ is the mean diffusion distance, a is the lattice spacing, n_s is the surface solute density, and ν is the molecular volume in the crystal. In Fig. 5a the growth data are plotted according to the logarithmic form of Eq. (5). This growth mechanism does not apply in the supersaturation range $1 < C/S < 3$, because a straight line should have been obtained. A surface nucleation mechanism has been observed with other solutes in a high-supersaturation regime (16,17). To test if the nucleation model for growth is correct at high supersaturation, the logarithm of Eq. (5) was fitted to the growth data for $C/S > 1.85$. From the slope of this line we obtained a value for γ of 0.86 $k_B T$. This is lower than the expected value in the range of 2.5 to 3.5 $k_B T$ (18).

In the case of a spiral growth mechanism, the presence of screw dislocations provides a perpetual source of steps on

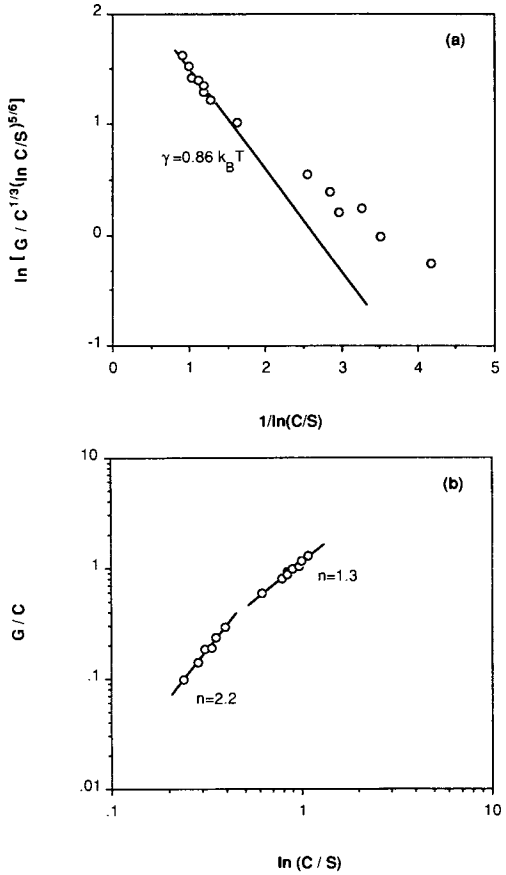

Fig. 5. Growth rate of theophylline monohydrate crystals at 10°C plotted according to (a) the surface nucleation model, Eq. (5), and (b) the screw dislocation model, Eq. (6). The surface nucleation model was fitted to the growth data at high supersaturation and γ was evaluated from the slope. The screw dislocation model predicts the data to fall on a line with slope $n = 2$ at low supersaturation and $n = 1$ at high supersaturation.

the surface. Burton, Cabrera, and Frank (BCF) developed a model which describes crystal growth by the addition of growth units to kink sites for a sequence of equidistant steps (19). The curvature of the spiral was related to the spacings of successive turns and to the level of supersaturation, and the steps are fed by a surface diffusion flux. The growth rate is given by

$$G = k_3 C[\ln(C/S)]^2 \quad (6)$$

where

$$k_3 = \frac{0.05\, D k_B T}{\gamma}.$$

At low supersaturations, Eq. (6) gives a rate of growth which is proportional to the square of the driving force and this relationship has been found to hold experimentally for many systems (14). At high supersaturations, the rate is proportional to the driving force and the step spacing is likely to be so close as to make direct capture at a kink site, from the supersaturated phase, possible without the need for surface diffusion. To compare Eq. (6) with experiments, we replotted the experimental data of Fig. 3 so that a straight line with slope $n = 2$ represents a fit to the expression, as shown in Fig. 5b. The value of n was determined to be 2.2 (standard error of 0.2) for low supersaturations and 1.3 (standard error of 0.1) for high supersaturations.

According to the BCF model the growth rate can change in a linear or parabolic way with the supersaturation, σ. In Fig. 6, we test the parabolic growth law by plotting ln G as a function of ln σ, according to the generalized expression

$$G = k_g \sigma^n. \quad (7)$$

The lines have been calculated by linear regression. The slope, n, is 2.2 (standard error of 0.2) at low supersaturations ($\sigma < 0.85$). These results are in agreement with the screw dislocation model. Values of the rate constant, k_g, were obtained from the slope of a plot of G as a function of σ^2 (Fig. 7). The values for n and k_g are summarized in Table I. At higher supersaturations $n = 1.5$ (standard error of 0.1), which may indicate a higher step density, where attachment of molecules to a step directly from the supersaturated phase is more probable than surface diffusion.

The temperature dependence of the growth rate constant is plotted according to the Arrhenius equation, $\ln k_g = \ln A - E_a/RT$, in Fig. 8. The energy of activation is not constant in the 10 to 40°C temperature range. A possible cause for this is that in evaluating k_g we have assumed that (a) theophylline is present in solution in monomeric form and (b) growth proceeds by attachment of monomers. However,

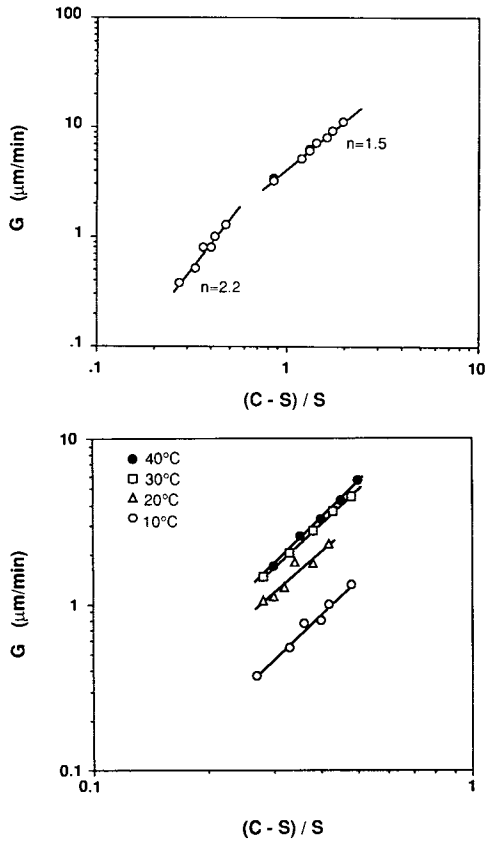

Fig. 6. Growth rate of theophylline monohydrate crystals plotted according to the power law, Eq. (7). The exponent, n, is evaluated from this plot.

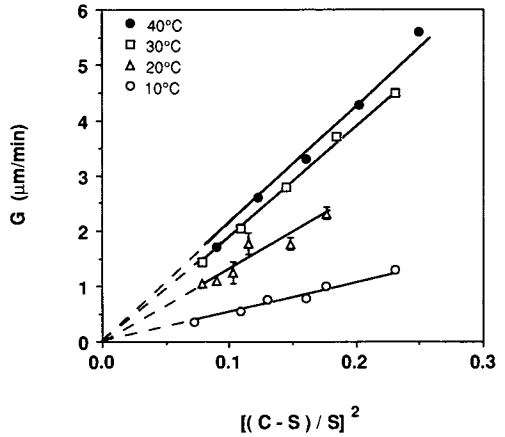

Fig. 7. Growth rate of theophylline monohydrate crystals plotted against the square of the supersaturation. The growth rate constant, k_g, is evaluated from this plot.

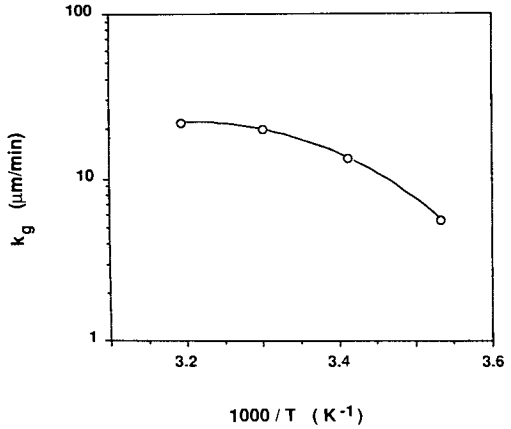

Fig. 8. Arrhenius plot of the growth rate constant of theophylline monohydrate crystals.

Nishijo *et al.* (19) have found that theophylline associates to form dimers and that this association occurs more readily when the molecules are in the unionized state and when the temperature is decreased. They evaluated the dimerization constant in the temperature range of 0 to 40°C and calculated an enthalpy change of −6.3 kcal/mol. How would this dimerization affect growth? If growth of theophylline monohydrate crystals is via monomers, the occurrence of aggregation would result in a weaker growth dependence on concentration. Thus, this assumption is valid, since the value of the growth rate constant is lower than that expected at the lower temperature (Fig. 8). Furthermore, the orientation of the molecules in the dimer (20) differs from the orientation of the theophylline molecules in the crystal lattice (21), rendering the dimer inactive for growth.

The temperature dependence of the growth rate constant may provide evidence for the rate-limiting step of the process. We compared the energy of activation for diffusion with the energy of activation for growth, in the temperature range of 10 to 20°C. The latter was determined by measuring the dissolution rate of theophylline monohydrate from a disk (22). The activation energy for diffusion is 4.4 kcal/mol, and that for crystal growth 14.3 kcal/mol. This confirms that growth of the monohydrate form is controlled by the surface reaction mechanism rather than by solute diffusion in the bulk.

Table I. Linear Regression Analysis Results of Growth Data in Figs. 6 and 7

T (°C)	n	k_g μm/min[a]
10[b]	1.50 (0.14)[c]	
10	2.20 (0.16)	5.47 (0.10)
20	1.99 (0.30)	13.0 (0.5)
30	2.13 (0.04)	19.5 (0.2)
40	2.27 (0.09)	21.5 (0.5)

[a] evaluated when $n = 2.0$.
[b] $\sigma > 0.85$.
[c] Standard error in parentheses.

In summary, the growth of theophylline monohydrate crystals is described by the BCF model, suggesting that the steps on the surface originate from screw dislocations. This is consistent with a rate of reaction that is proportional to the square of the driving force. The growth rate is independent of the stirring rate and the activation energy for growth is larger than the value for simple diffusion. It thus appears that although diffusion is the mechanism controlling the dissolution of crystals, growth is controlled by a surface reaction.

ACKNOWLEDGMENT

This work was supported in part by a Biomedical Research Support Grant at the University of Arizona.

REFERENCES

1. E. Shefter, H. Fung, and O. Mok. Dehydration of crystalline theophylline monohydrate and ampicillin trihydrate. *J. Pharm. Sci.* 62:791–794 (1973).
2. D. A. Wadke and G. E. Reier. Use of intrinsic dissolution rates to determine thermodynamic parameters associated with phase transitions. *J. Pharm. Sci.* 61:868–871 (1972).
3. P. Kahela, R. Aaltonen, E. Lewing, M. Anttila, and E. Kristoffersson. Pharmacokinetics and dissolution of two crystalline forms of carbamazepine. *Int. J. Pharm.* 14:103–112 (1983).
4. E. Laine, V. Tuominen, P. Ilvessalo, and P. Kahela. Formation of dihydrate from carbamazepine anhydrate in aqueous conditions. *Int. J. Pharm.* 20:307–314 (1984).
5. E. Shefter and T. Higuchi. Dissolution behavior of crystalline solvates and nonsolvated forms of some pharmaceuticals. *J. Pharm. Sci.* 52:781–791 (1963).
6. E. Shefter and G. Kmack. Preliminary study of theophylline hydrate-anhydrate system. *J. Pharm. Sci.* 56:1028–1029 (1967).
7. J. H. de Smidt, J. G. Fokkens, H. Grijseels, and D. J. A. Crommelin. Dissolution of theophylline monohydrate and anhydrous theophylline in buffer solutions. *J. Pharm. Sci.* 75:497–501 (1986).
8. J. Herman, J. P. Remon, N. Visavarungroj, J. B. Schwartz, and G. H. Klinger. Formation of theophylline monohydrate during pelletisation of microcrystalline cellulose-anhydrous theophylline blends. *Int. J. Pharm.* 42:15–18 (1988).
9. J. Herman, N. Visavarungroj, and J. P. Remon. Instability of drug release from anhydrous theophylline-microcrystalline cellulose formulations. *Int. J. Pharm.* 55:143–146 (1989).
10. E. Suzuki, K. Shimomura, and K. Sekiguchi. Thermochemical study of theophylline and its hydrate. *Chem. Pharm. Bull.* 37:493–497 (1989).

11. S. Byrn. *Solid State Chemistry of Drugs,* Academic Press, New York, 1982, pp. 156, 178.
12. C. Misra and E. T. White. Kinetics of crystallization of aluminum trihydroxide from seeded caustic aluminate solutions. *AIChE* 67:53–65 (1971).
13. M. Ohara and R. C. Reid. *Modeling Crystal Growth Rates from Solution,* Prentice–Hall, Englewood Cliffs, NJ, 1973, pp. 47–48.
14. G. H. Nancollas. The growth of crystals in solution. *Adv. Colloid Interface Sci.* **10**:215–252 (1979).
15. J. D. Weeks and G. H. Gilmer. Dynamics of crystal growth. *Adv. Chem. Phys.* **40**:157–228 (1979).
16. N. Rodriguez-Hornedo and S. D. Durbin. Crystallization mechanism and kinetics of human insulin. *Pharm. Res.* **6**:S151 (1989).
17. J. Garside. Advances in the characterization of crystal growth. *AIChE Symp. Ser.* **80**:23–38 (1984).
18. W. K. Burton, N. Cabrera, and F. C. Frank. The growth of crystals and the equilibrium structures of their surfaces. *Phil Trans. Roy. Soc.* **A243**:299–358 (1951).
19. P. Bennema and O. Sohnel. Interfacial surface tension for crystallization and precipitation from aqueous solutions. *J. Crystal Growth.* **102**:547–556 (1990).
20. J. Nishijo, I. Yonatani, K. Tagahara, Y. Suzuta, and E. Iwamoto. Influence of temperature and ionization on self-association of theophylline in aqueous solution. *Chem. Pharm. Bull.* **34**:4451–4456 (1986).
21. J. Sutor. The structure of pyrimidines and purines. VI. The crystal structure of theophylline. *Acta Cryst.* **11**:83–87 (1958).
22. H. J. Wu. *The Kinetics of Solvent Mediated Phase Transformations,* Ph.D. thesis, University of Arizona, Tucson, 1989.